Research paper

Load capacity of steel-aluminium brackets under static and cyclic laboratory tests

A. Ambroziak[1]

Abstract: The aim of the research is the laboratory investigation of steel-aluminium brackets employed to fasten lightweight curtain walls to building facilities. Static pressure, suction forces, and cyclic loads parallel to end plates (horizontal – to simulate wind influence) were applied in the study. The steel-aluminium brackets were tested on a reinforced concrete substrate made of C30/37 concrete class to simulate the real working conditions. Laboratory tests were performed to failure of the brackets or damage of anchoring fastened to the concrete elements. Additionally, the tensile capacity of stainless steel bolt connections screwed in aluminium profile was determined. The uniaxial tensile tests were performed for three length variants of the anchorage: 28 mm, 14 mm, and 7 mm of the stainless steel bars screw-in in threading aluminium profiles. In the course of cyclic tests, a hinge formed in the location of bolt connections made the change of the working character of steel-aluminium brackets. The cyclic tests also showed the danger of the strap aluminium profile displacement due to improper connection with the main aluminium profile. The paper is intended to provide scientists, civil engineers, and designers with an experimental assessment of mechanical properties of steel-aluminium brackets under static and cyclic loads.

Keywords: steel-aluminium bracket, mechanical properties, EN AW-6060 T66, curtain walls, mullion-transom facade

[1] DSc., PhD., Eng., Prof. GUT, Gdansk University of Technology, Faculty of Civil and Environmental Engineering, St. Gabriela Narutowicza 11/12, 80-233 Gdańsk, Poland, e-mail: ambrozan@pg.edu.pl, ORCID: https://orcid.org/0000-0002-7735-7863

1. Introduction

The mullion-transom facade is the most widespread system for building glass facades (see e.g. [11], [19]). Structural and functional requirements for curtain walling are specified in PN-EN 13830 [20], see also [9]. Classical, vertical division of the panels and free architectural forms are widely applied in curtain wall facades. The horizontal and vertical elements are made of extruded aluminium profiles (EN AW-6060 T66 aluminium alloy [7]). The mullions (vertical elements) are fixed to the load-bearing structure by brackets. The brackets are made of aluminium, steel or mixed materials (e.g. steel-aluminium). The design of the mullion-transom facades is generally based on existing system solutions available on the building market. Each facade system is limited, having some advantages and disadvantages which influence the costs of facade system implementation (see e.g. [13], [17], [18]). Some projects introduce systems of individual solutions (see e.g. [2]) to meet the challenges of designed modern and extraordinary buildings (see e.g. [5], [4], [14]). Individual solutions require additional structural analysis (see e.g. [1], [6]) and laboratory tests (see e.g. [3], [16], [12]) to avoid design or construction problems and defects during the exploitation (see e.g. [15], [21]). The research aims to estimate the load capacity of steel-aluminium bracket used to fasten lightweight curtain walls to building facilities (see Fig. 1). In order to assure specified load-capacity the static and cyclic laboratory tests were carried out. The investigation contributes an expert opinion on the bearing capacity of steel-aluminium bracket and the possibilities of carrying design loads and assuring the required working life. The paper provides scientists, engineers, and designers with an experimental assessment of mechanical properties of steel-aluminium bracket under static and cyclic loads.

Fig. 1. View on fixed steel-aluminium brackets in mullion-transom wall system
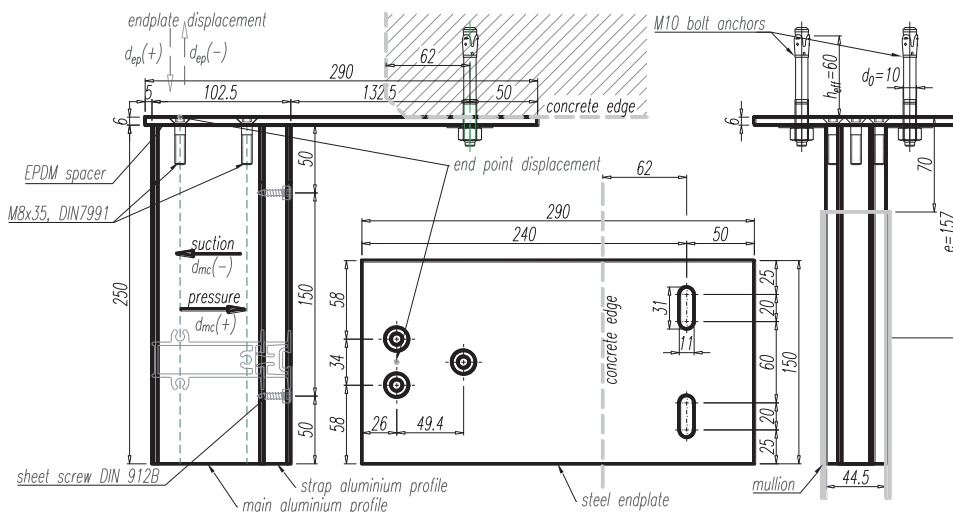
Fig. 2. View and cross-section of analysed steel-aluminium bracket

Table 1. Technical data of a single anchor in non-cracked normal concrete, see [10]

parameters and units	values
Nominal drill hole diameter d_0 [mm]	10
Effective anchorage depth h_{ef} [mm]	60
Installation torque T_{inst} [Nm]	45
Steel failure – characteristic resistance $N_{Rk,s}$ [kN]	27.2
Pullout failure – characteristic resistance in uncracked concrete C30/37 $N_{Rk,p}$ [kN]	19.52

2. Materials

The investigated steel-aluminium bracket consists of a hot deep galvanized steel S355 endplate of 6 mm thickness and EN AW-6060 T66 aluminium alloy element connected by three steel bolts (A2-70 stainless steel bolts M8x35, DIN 7991), see Fig. 2. Two oval holes in the end plate are provided to fasten the bracket to the building structure and three conical holes to connect with the aluminium profile. Between hot deep galvanized steel endplate and aluminium profiles, the EPDM spacer is applied. The aluminium profile is composed of two units: the main element and the strap. The strap profile is connected to the main aluminium profile by two steel screws A2-70 5.5x19 (sheet screw DIN 912B). The steel-aluminium bracket is fastened to the reinforced concrete structure by two M10 bolt anchors (see Table 1) installed in a drilled hole in a reinforced concrete element (strength class C30/37, see [8]) and anchored by torque-controlled expansion.
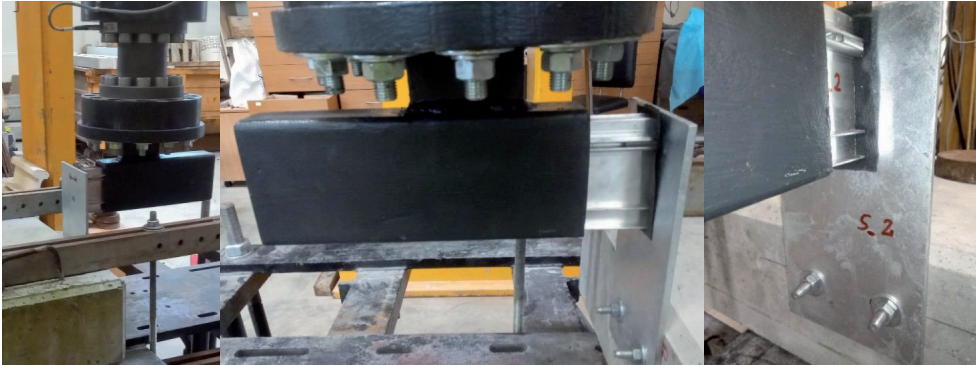
Fig. 3. View on laboratory test stand

3. Laboratory tests

3.1. Test of brackets under monotonic loading

The loads parallel to the endplate are applied in laboratory tests by means of the computer-controlled Zwick testing machine (see Fig. 3). The rectangular steel element connected to the movable crosshead of the testing machine represents the mullion. The internal cross-section of the rectangular steel element (45×103.5mm) is an exact representation of the aluminium mullion used in a mullion-transom wall system. The aluminium profile of the steel-aluminium bracket (see Figs. 2 and 3) is slid into the rigid rectangular steel element. The loads are applied as tensile and compressive forces to simulate the wind impact (suction (-) and pressure (+), see Fig. 2) on the mullion-transom façade system. The brackets are subjected to pressure or suction with a force-controlled constant loading speed equal to 100 N/s. The laboratory experiments are performed with a constant loading speed to failure of the brackets or damage of the anchoring fastened to the concrete. The force held every 1 kN in its 60 s waiting time when the displacement of the endplate is monitored. All tests are performed at room temperature (about 20°C). The bracket is intended to carry loads in the designed force range +5 ÷ -5 kN. Six steel-aluminium brackets are tested, three under pressure loading and three under suction loading.

Forces at rupture (F_R) and displacements of the movable crosshead of the testing machine d_{mc}^R and endplate d_{ep}^R at rupture obtained in the steel-aluminium bracket laboratory tests are shown in Table 2. The mean values and standard error of the mean of the specified range are also given. It should be noted, that in the case of pressure forces the damage of aluminium profile and a significant distortion

of steel bolts are observed, see Fig. 4a. Each main aluminium profiles under pressure loading in the bolt connection place are significantly deformable, see Fig. 5. On the other hand, in the suction case, the rupture forces are determined by the strength of bolt anchoring (damage of edge concrete), see Fig. 4b. Distortion of steel bolts is observed too. The mean rupture forces are nearly equal for pressure and suction cases (only 3% differences are observable, see Table 2). The force vs displacement of movable crosshead (d_{mc}) diagram and the force vs endplate displacement (d_{ep}) diagram up to rupture of the steel-aluminium bracket are shown in Figs. 6 and 7.

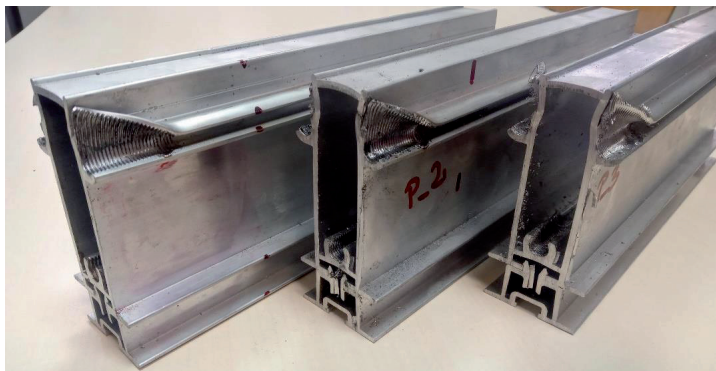Fig. 4. Form of bracket failure: a) left – pressure, b) right – suction

Fig. 5. Form of aluminium profile failure under pressure loading

Table 2. Forces and displacements at rupture of steel-aluminium bracket

	pressure			suction		
	F_R [kN]	d_{mc}^R [mm]	d_{ep}^R [mm]	F_R [kN]	d_{mc}^R [mm]	d_{ep}^R [mm]
Test 1	19.95	17.34 (15.26^{+1kN})	2.40 (1.43^{+1kN})	-23.01	-15.39	-1.95 (-2.03^{MAX})
Test 2	22.98	20.42 (17.62^{+1kN})	2.67 (1.07^{+1kN})	-21.01	-12.87	-1.73 (-1.95^{MAX})
Test 3	22.01	18.40 (14.91^{+1kN})	3.22 (1.17^{+1kN})	-23.00	-13.07	-1.47 (-1.75^{MAX})
mean	21.6 ± 0.9	18.7 ± 0.9 $(15.9 \pm 0.8^{+1kN})$	2.8 ± 0.2 $(1.2 \pm 0.1^{+1kN})$	-22.3 ± 0.7	-13.8 ± 0.8	-1.7 ± 0.1 (-1.9 ± 0.1^{MAX})

At the start of the pressure loadings a significant slide in displacements is observed (small diagrams in Figs. 6a and 7a). It can be explained by slackness of the aluminium profile embedded in the rectangular steel profile. Therefore it is decided to show the graphs corresponding to 1 kN force with a zero displacement. Additionally, in the case of suction after exceeding the -5 kN loading (tests: s_t2 and s_t3, see Fig. 7b) the endplate displacement is highly nonlinear. The loss of load-bearing occurs in the screw joint, the endplate displacements are decreased to failure. Under pressure loading, the displacement d_{mc} (see Fig. 6a) shows nonlinear character while the force is greater than 10kN. Above observable limits, deformations of aluminium profile in the anchorage of steel bolts were detected. The endplate reached (see Figs. 7a and 7b) about 2 mm displacement only despite the loads over 20kN. It can be concluded that the base plate is sufficiently stiffened and the anchoring fulfils capacity requirements.
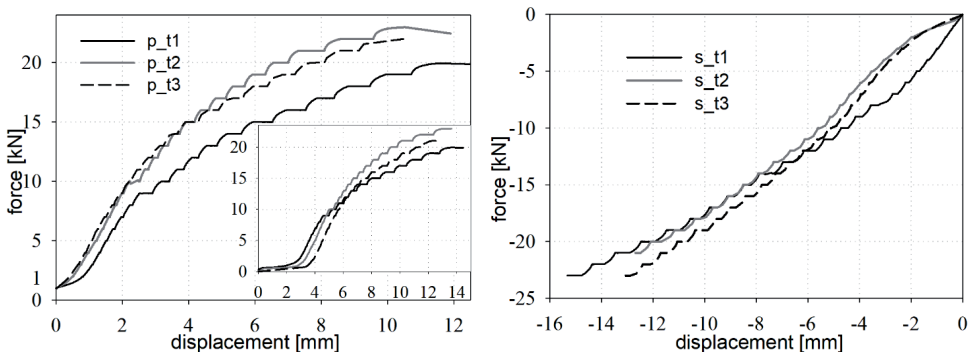

Fig. 6. Force versus movable crosshead displacement: a) pressure, b) suction
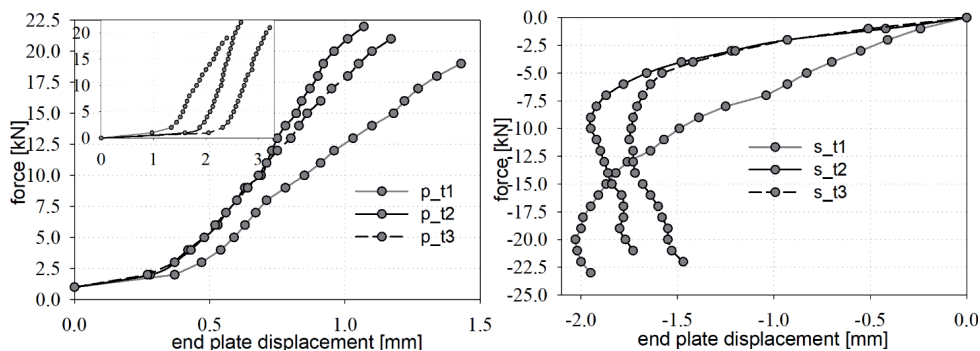
Fig. 7. Force versus endplate displacement: a) pressure, b) suction

3.2. Test of brackets under cyclic loading

In the next laboratory work stage, the cyclic tests are carried out to analyse variations of steel-aluminium bracket capacity. The cyclic force-controlled tests are carried out up to failure at room temperature (about 20°C). Five steel-aluminium brackets are subjected to cyclic loadings (variable loading sign: pressure or suction) with a force-controlled constant loading speed equal to 1000 N/s up to failure. The cyclic tests are performed due to every load increase equal to 5 kN (level L1: +5/-5 kN; level L2: +10/-10 kN; level L3: +15/-15 kN; level L4: +20/-20 kN), see Fig. 8. The used denotations c_t1_L1 means: c – cyclic test, t1 – specimen number, L1 – load level, respectively. Fifty cycles are performed at each level of loadings. The force is held in every upper and lower reversal point cycle at 5 s waiting time while the displacement of the endplate is monitored.

Failure of all brackets during cyclic tests occurs under pressure loading, see Fig. 10. Like in static pressure loading the aluminium profile is highly deformed and failure occurs in the aluminium profile in bolt connections place (compare Fig. 10 and Fig. 6). The maximum/minimum endplate displacements for specified cycle numbers are shown in Fig. 9. The used denotations c_t1_p or c_t1_s means: c – cyclic test, t1 – specimen number, p – pressure load, or s – suction load, respectively. Three brackets are damaged during the L3 level of cyclic loading, two of them fail during the first cycle of the L4 loading level (the first increase of loading after the L3 level), see Figs. 8 and 9. In the course of cyclic tests this defect is linked with a displaced bottom aluminium profile (strap aluminium profile), see Fig. 10. The greatest displacement of strap aluminium profiles is observed for c_t4 and c_t5 tests.
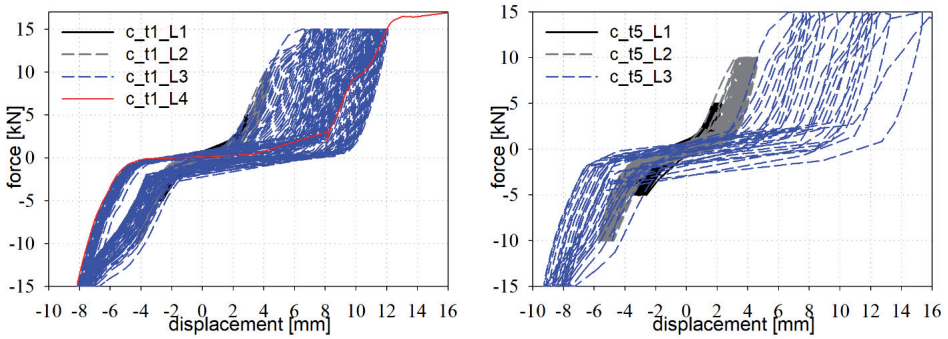
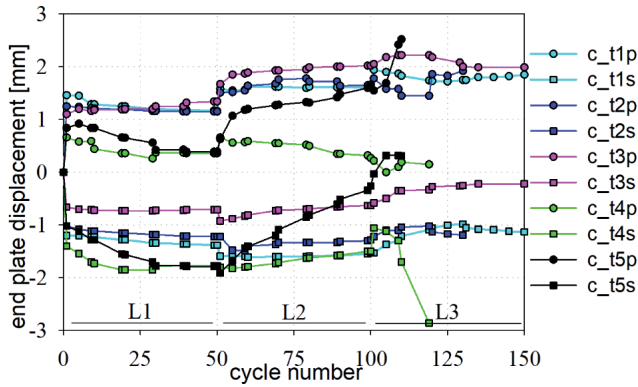Fig. 8. Cyclic tests - force versus displacement of movable crosshead

Fig. 9. Maximum/minimum endplate displacement versus cycle number

Fig. 10. Form of bracket failure under cyclic tests – visible displace of bottom aluminium profile
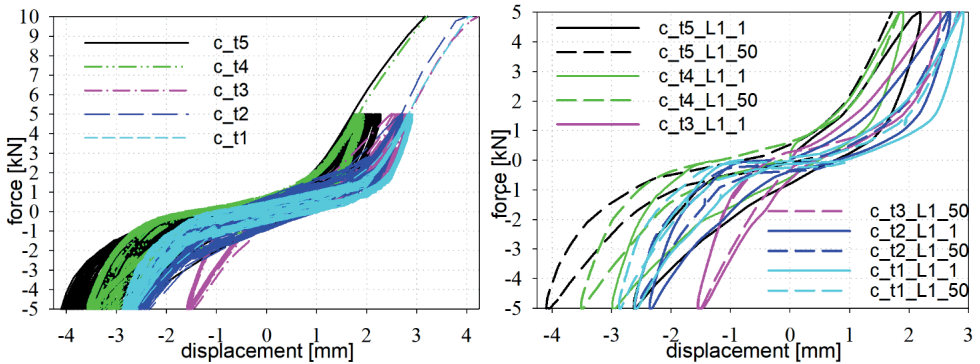
Fig. 11. Force versus displacement of movable crosshead

Table 3. Maximum/minimum displacements [mm] of movable crosshead obtained for cycle number

	c_t1	c_t2	c_t3	c_t4	c_t5	mean
L1_1p	2.91	2.69	2.53	1.91	2.20	**2.45 ± 0.18**
L1_50p	2.81	2.69	2.85	1.84	1.71	**2.38 ± 0.25**
L2_1p	4.12	4.02	4.31	3.27	3.24	**3.79 ± 0.22**
L1_1s	-2.61	-2.36	-1.55	-2.99	-2.63	**-2.43 ± 0.24**
L1_50s	-2.87	-2.61	-1.54	-3.51	-4.10	**-2.93 ± 0.43**

Table 4. Maximum/minimum endplate displacements [mm] obtained for cycle number

	c_t1	c_t2	c_t3	c_t4	c_t5	mean
L1_1p	1.46	1.25	1.10	0.66	0.84	**1.06 ± 0.14**
L1_50p	1.16	1.15	1.34	0.36	0.39	**0.88 ± 0.21**
L2_1p	1.58	1.51	1.67	0.66	0.63	**1.21 ± 0.23**
L1_1s	-1.20	-1.02	-0.66	-1.40	-1.02	**-1.06 ± 0.12**
L1_50s	-1.38	-1.22	-0.71	-1.77	-1.79	**-1.37 ± 0.20**

Displacements of the endplate (Fig. 9) and the movable crosshead (Fig. 11) are different according to the tests, showing significant displacements of a bottom aluminium profile (strap aluminium profile). The used denotations in Fig. 11, e.g.: c_t1_L1_50 means: c – cyclic test, t1 – specimen number, L1 – load level, 50 – cycle number, respectively. The numerical results of movable crosshead displacements and endplate displacements for the 1st and 50th cycles number of level L1 (L1_1, L1_50

where: p – pressure load, or s – suction load) and 1st pressure cycle of level L2 (L2_1) are collected in tables 3 and 4. The mean endplate displacements are 2-3 times lower than mean movable crosshead displacements. The displacements under pressure for the 50th cycle are less than the values obtained for the 1st cycle (3% for movable crosshead displacement and 17% for endplate displacement, see tables 3, 4). On the other hand under suction loading, the displacements for the 50th cycle are higher than the ones obtained for the 1st cycle (20-30%, see tables 3, 4). During cyclic tests when the forces exceed the first loading level significant deformation of the aluminium profile in bolt connection place is observed, see Fig. 12. A hinge is formed at the bolt connection. For this reason, despite the significant increase in the movable crosshead displacements, the displacements of the endplate do not increase significantly.
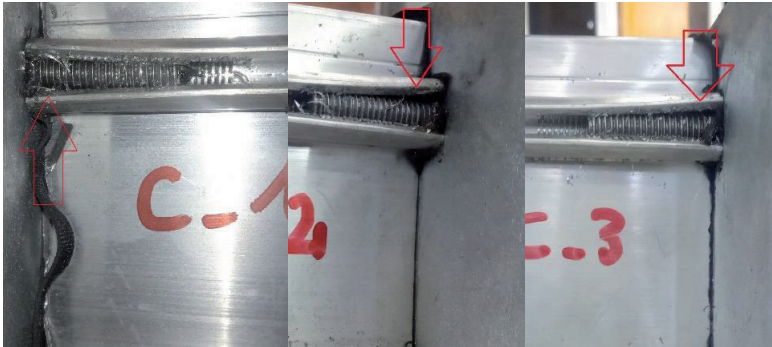

Fig. 12. Deformation of aluminium profile in bolt connection place

Fig. 13. Investigated bolt connections: a) view on specimens, b) clamped in a testing machine grips

3.2. Tensile capacity of steel bolt connections

Tensile capacity of the stainless steel bolt connections screwed in aluminium profile is determined. The connection specimens in the form of the steel-aluminium brackets are manufactured and delivered to the laboratory by a contractor of building glass facades. The A2-70 stainless steel bolts M8 in steel-aluminium bracket are screwed-in aluminium profile on about 28 mm, see Fig. 2. The laboratory investigated aluminium profile is both-side threaded before the steel bars are fastened. Uniaxial tension tests are performed for three length variants (anchorage of 28 mm, 14 mm, and 7 mm) of the A2-70 stainless steel M8 bars screwed in threaded aluminium profiles, see Fig. 13. From one side the steel bars were screw-in on the specific length, from another side the anchorage of steel bars was about 40 mm. Three specimens are investigated for each length. The connections are subjected to tensile loadings with a constant displacement speed (displacement controlled) equal 5 mm/min.
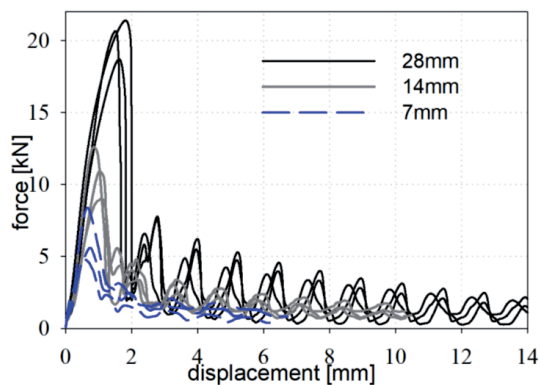

Fig. 14. Results of bolt connections capacity: force versus displacement

Table 5. Maximal forces under tension loadings

	28 mm	14 mm	7 mm
Specimen 1	20.66	12.61	8.39
Specimen 2	18.70	9.02	5.69
Specimen 3	21.39	10.93	4.78
mean	**20.3 $\pm$ 0.8**	**10.9 $\pm$ 1.0**	**6.3 $\pm$ 1.1**

The mean shear thread strength determined by the maximum tensile forces in the aluminium profile is equal to 20.3 kN for 28 mm, 10.9 kN for 14 mm and 6.3 kN for 7 mm, the lengths denote anchorage of steel bars. The mean maximum tension forces obtained during laboratory tests may be regarded as proportional to the screwed-in steel bars length, see table 5. A wide scatter in individual tensile forces may be produced by minor inaccuracies of threading the aluminium profile to anchorage steel bolts. The results of tension tests (force versus displacement graphs) are shown in Fig. 14. The slip of bars anchorage in the aluminium profile thread is observed under maximum forces. Nevertheless, the next force picks, slips occur, thus the connections can transfer decreased tensile loadings (see Fig. 14) to reach the final loss of tension loading capacity. The threaded aluminium profile undergoes plastic deformations on the surface of steel bar contacts during slips and the shear thread strength in the aluminium profile is reached.

Based on the laboratory test results it is possible to preliminary estimate the force P_{max} which can be applied to the investigated steel-aluminium bracket. Multiplying the mean maximum force (20.3 kN, see table 5) by the spacing of stainless steel bolts M8 (4.94 cm, see Fig. 2) maximum pure bending moment under suction loading results M^s_{max} =100.282 kNcm (20.3 kN × 4.94 cm). Assumed that the load is transferred by mullion to the aluminium profile at a uniform rate it can the position of a resultant force acting on the bracket may be specified (e = 15.7 cm, see Fig. 2). The force P^s_{max} under suction causing to reach the shear thread strength in the aluminium profile equals P^s_{max} = 6.3 kN (100.282 kNcm/15.7 cm). The estimated force under pressure loading is equal to P^p_{max} = 12.6 kN (2 ×6.3 kN). These estimated forces are slightly greater than the static suction and pressure working capacity loads (5 kN, and 10 kN specified under monotonic loading), respectively. Nevertheless, the estimated forces P^s_{max} and P^p_{max} are much smaller (two-three times) than determined forces at rupture (F_R, see Table 2). The steel endplate is relatively rigid and the bolts in connections are subjected to combined tensile, bending and, shear (see Figs. 4 and 10). The capacity of the bolt connections in connection main aluminium profile with steel endplate can be specified generally by the sum of the shear capacity of the connection and tensile. The tensile capacity of the bolt connection may be used to estimation of the bolt connection capacity in the elastic range working (working capacity loads).

4. Discussion and conclusions

The investigation is aimed at assessing the load resistance of a steel-aluminium bracket under static and cyclic loadings. In the course of pressure and suction deformation of the aluminium profile is

observed, the length of the mating threads decreases. Under cyclic tests the hinge is formed in bolt connections, changing the working character of steel-aluminium brackets. The cyclic tests exhibit the possibilities of the strap aluminium profile displacement due to improper connection with the main aluminium profile. Significant slips of strap aluminium profile change the deformation character of the investigated bracket because the position of a resultant force acting on the aluminium profile is changed and consequently affecting to bolt connection working. Based on the performed laboratory tests the following conclusions may be drawn:

- The tension forces specified under laboratory tests for steel bolt connection to the main aluminium profile may be regarded as proportional to the screwed-in steel bars length. The slip of bars anchorage in the aluminium profile thread is observed before it completely loses its tension loading capacity.

- The steel-aluminium bracket may carry out static and cyclic loads safely in the designed force range +5 ÷ -5 kN. In the engineering application, it is recommended to apply an additional safety factor to maintaining an appropriate level of safety.

- To ensure the blockade of the strap aluminium profile sliding and proper connection with the main aluminium profile, it is recommended to provide a screw-in connection of three stainless steel 5.5x3.8 self-drilling screws (DIN7504N). New laboratory tests should be performed to specify the impact of an additional blockade of the strap aluminium profile on steel-aluminium bracket behaviour under loading.

- To fulfil the required load-bearing capacity of the connection endplate with an aluminium profile by bolts fixing, the quality of the carried out thread in aluminium profile should be improved. In this regard, the manufacturer should afford to take the Factory Production Control procedure verified.

The paper may be considered a possible base for new investigations. The obtained results encourage the author to continue the research, based on cycle tests with a high number of cycles and creep tests to confirm specified limits of load capacity. The future research will be also supplemented with numerical analysis of the tested bracket. The author hopes that the described laboratory tests spark a vital interest in the community of civil engineers and scientists to take into consideration the subject of the load-bearing capacity of steel-aluminium brackets applied to fastened mullion-transom façades in building structures.

References

[1] G. Akhmadullina and G. Shmelev, "Numerical modeling and optimization of geometric parameters of a composite bracket," *IOP Conf. Ser. Mater. Sci. Eng.*, vol. 890, pp. 012051, 2020. https://doi.org/10.1088/1757-899X/890/1/012051

[2] Aluprof, Projekt Specific & Bespoke Solutions, (n.d.). https://aluprof.eu/files/downloads/katalog%20_rozwiazan_indywidualnych(kri)pl_en.pdf (accessed July 29, 2020)

[3] A. Ambroziak, "Mechanical Properties of Aluminium Bracket Strengthening," Arch. Civ. Eng. 65 (2019) 203–216. https://doi.org/10.2478/ace-2019-0055

[4] T. Z. Błaszczyński, "Ekologiczne wieżowce," *Builder*, vol. 262, no. 5, pp. 86–89, 2019. http://dx.doi.org/10.5604/01.3001.0013.3610

[5] M. Brzezicki, "Glass protected timber façades – new sustainable façade typology," *Tech. Trans.*, vol. 5, pp. 5–22, 2019. https://doi.org/10.4467/2353737XCT.19.050.10574

[6] L. Casagrande, A. Bonati, F. Auricchio and A. Occhiuzzi, Dissipating effect of glazed curtain wall stick system installed on high-rise mega-braced frame-core buildings under nonlinear seismic excitation, in: *COMPDYN 2017 - Proc. 6th Int. Conf. Comput. Methods Struct. Dyn. Earthq. Eng.*, 2017, pp. 3711–3727. https://doi.org/10.7712/120117.5677.17166

[7] CEN (European Committee for Standardization), EN 755-2: Aluminium and aluminium alloys. Extruded rod/bar, tube and profiles - Part 2: Mechanical properties, (2016).

[8] CEN (European Committee for Standardization), "EN 206:2013+A1:2016 Concrete -- Specification, performance, production and conformity," 2016, pp. 1-74.

[9] M. Cwyl, "Podstawowe wymagania normowe współczesnych ścian metalowo-szklanych," *Inżynieria i Bud.*, vol. 69, no. 6, pp. 305–307, 2013.

[10] DIBt (Deutsches Institut für Bautechnik), "ETA-05/0069 fischer Bolt Anchor FAZ II. Torque controlled expansion anchor of sizes M8, M10, M12, M16, M20 and M24 for use in concrete," 2016, pp. 1–21.

[11] O. Fedorov and V. Lazina, Modern translucent enclosures in architecture, Archit. Eng. 4 (2019) 12–21. https://doi.org/10.23968/2500-0055-2019-4-4-12-21

[12] A. V. Galyamichev, V. A. Kirikova, G. E. Gerasimova and A. Sprince, "Bearing capacity of facade systems fixing to sandwich panels," *Mag. Civ. Eng.*, vol. 78, pp. 30–46, 2018. https://doi.org/10.18720/MCE.78.3

[13] M. Górka and A. Leśniak, Systemy fasad aluminiowo–szklanych i ich ocena wielokryterialna, Zesz. Nauk. Politech. Częstochowskiej. Bud. 174 (2018) 102–107. https://doi.org/10.17512/znb.2018.1.16

[14] M. Jaworska-Michałowska, "Szklane fasady w budynkach kształtowanych przez klimat – wybrane zagadnienia," *Przegląd Bud.*, vol. 7-8, pp. 43–46, 2010. https://www.przegladbudowlany.pl/2010/07-8/2010-7-8-PB-43-46_Jaworska.pdf

[15] K. Kazmierczak, "Review of curtain walls, focusing on design problems and solutions," in: *Build. Enclos. Sci. Technol.*, Portland, USA, 2010: pp. 1–20. https://cdn.ymaws.com/www.nibs.org/resource/resmgr/best/best2_008_ee4-1.pdf

[16] M. Kołaczkowski and A. Byrdy, FEM Analysis and Experimental Research into Carrier Brackets in Ventilated Facades, Period. Polytech. Civ. Eng. (2020) 1–9. https://doi.org/10.3311/ppci.13822

[17] A. Leśniak and M. Górka, Structural Analysis of Factors Influencing the Costs of Facade System Implementation, Appl. Sci. 10 (2020) 6021. https://doi.org/10.3390/app10176021

[18] A. Leśniak, D. Wieczorek and M. Górka, Costs of facade systems execution, *Arch. Civ. Eng.*, vol. 66, no. 4, pp. 81–95, 2020. https://doi.org/10.24425/ace.2020.131776

[19] D. D. Mijovic, D. Milanovic and S. Jelena, "Curtain walls: history and a continuing challenge," in: *XVIII Int. Sci. Conf. "Construction Archit. VSU 2018*, Sofia, Bulgaria, 2018, pp. 1–6.

[20] PKN (Polish Committee for Standardization), "PN-EN 13830 Curtain walling. Product standard," 2020, pp. 1- 92.

[21] J. Č. Tovarović, N. Šekularac and J. Ivanović-Šekularac, "Problems Associated With Curtain Walls," *Struct. Eng. Int.*, vol. 27, pp. 413–417, 2017. https://doi.org/10.2749/101686617X14881937385322

Nośność konsol stalowo-aluminiowych na podstawie statycznych i cyclicznych badań laboratoryjnych

Streszczenie:

Przedmiotem przedstawionych w artykule badań laboratoryjnych są konsole stalowo-aluminiowe, które są stosowane jako elementy łącznikowe fasad słupowo-ryglowych z konstrukcją budynku. Blacha podstawy konsoli wykonana jest ze stali S355, która jest połączona z profilem aluminiowym ze stopu aluminium EN AW-6060 T66 [7] trzema nierdzewnymi śrubami A2-70 M8x35 (DIN 7991). Pomiędzy blachą podstawy a profilem aluminiowym zastosowana jest przekładka z EPDM-u. Konsole stalowo-aluminiowe poddawane były statycznym próbom obciążenia siłami parcia i ssania, które symulowały obciążenia wiatrem. Konsola w trakcie badań zamocowana była do elementów żelbetowych wykonanych z betonu C30/37 dwoma kotwami sworzniowymi M10 z kontrolowanym momentem dokręcenia. Wyznaczone siły niszczące dla obciążeń pochodzących od parcia (21.6 ± 0.9 kN) i ssania (-22.3 ± 0.7 kN) mają podobne wartości, przy czym o nośności konsoli na obciążenia pochodzące od ssania decydowała nośność zakotwienia (które uległo zniszczeniu przy tym poziomie obciążenia). Oprócz badań statycznych przeprowadzono badania cykliczne, w których obciążenie przykładane było naprzemiennie jako parcie i ssanie dla następujących poziomów obciążenia: L1 (+5/-5 kN), L2 (+10/-10 kN), L3 (+15/-15 kN), L4 (+20/-20 kN). Dla każdego poziomu obciążenia konsole poddawane były 50 cyklom obciążenia. Trzy z badanych konsol uległy zniszczeniu podczas badań cyklicznych przy poziomie L3 oraz dwie konsole przy przekroczeniu obciążenia +15 kN (początek poziomu L4). Na podstawie badań cyklicznych stwierdzono możliwość wysuwania się dolnego profilu aluminiowego, który jest dołączany do głównego profilu za pomocą dwóch wkrętów. W celu wyeliminowania przemieszczania się dolnego profilu zalecono połączenie trzema blachowkrętami samowiercącymi z łebkiem walcowym ze stali nierdzewnej 5.5x3.8 (DIN7504N). Przeprowadzone badania wytrzymałościowe potwierdziły możliwość przeniesienia projektowanych obciążeń w zakresie +5 ÷ -5 kN.

Jednym z elementów decydujących o nośności konsoli stalowo-aluminiowej jest nośność połączenia wkręconych w nagwintowany profil aluminiowy śrub M8. W celu oszacowania nośności tego połączenia wykonano testy jednoosiowego rozciągania połączenia pręta M8 wkręcanego w nagwintowany profil aluminiowy na określone długości (28 mm, 14 mm i 7 mm). Nośność tego połącznia jest proporcjonalna do długości wkręcania pręta/śruby w profil aluminiowy. Oszacowania na tej podstawie nośność konsoli jest wyższa niż otrzymana na podstawie badań wytrzymałościowych. Wynika to z faktu, iż na połączenie śrubowe oddziaływają nie tylko obciążenia rozciągające, ale także ścinające i zginające.